ICES Journal of
Marine Science

ICES Journal of Marine Science (2021), 78(9), 3464–3476. https://doi.org/10.1093/icesjms/fsab158

## Original Article

# Population connectivity of the euphausiid, *Stylocheiron elongatum*, in the Gulf Stream (NW Atlantic Ocean) in relation to COI barcode diversity of *Stylocheiron* species

Ann Bucklin [1,*], Jennifer M. Questel[2], Leocadio Blanco-Bercial [3], Alexandra Frenzel[1],
Sara B. Smolenack[4], and Peter H. Wiebe [5]

[1]*University of Connecticut, Groton, CT 06340, USA*
[2]*University of Alaska Fairbanks, Fairbanks, AK 99775, USA*
[3]*Bermuda Institute of Ocean Sciences, St. George's, GE 01, Bermuda*
[4]*University of New Hampshire, Durham, NH 03824, USA*
[5]*Woods Hole Oceanographic Institution, Woods Hole, MA 02543, USA*

**Corresponding author: tel: +1 860-405-9260; e-mail: ann.bucklin@uconn.edu*

Bucklin, A., Questel, J. M., Blanco-Bercial, L., Frenzel, A., Smolenack, S. B., and Wiebe, P. H. Population connectivity of the euphausiid, *Stylocheiron elongatum*, in the Gulf Stream (NW Atlantic Ocean) in relation to COI barcode diversity of *Stylocheiron* species. – ICES Journal of Marine Science, 78: 3464–3476.

Received 9 January 2021; revised 23 July 2021; accepted 3 August 2021; advance access publication 26 August 2021.

The euphausiid genus *Stylocheiron* includes species with biogeographical distributions spanning multiple ocean basins. Despite their circumglobal distributions, the species show low levels of genetic diversity and little or no evidence of population structure based on the mitochondrial cytochrome oxidase I (COI) barcode region, with the exception of a possible cryptic species within *Stylocheiron affine*. *Stylocheiron elongatum* showed $<$ 1% variation of the COI barcode region among populations in different ocean basins, but analysis of samples collected from the Florida Current (February, 1993) and Gulf Stream Meander Region (April, 1993) in the Northwest Atlantic Ocean revealed small-but-significant genetic differentiation between samples based on a different section of COI and mitochondrial cytochrome b (CYB). Both COI and CYB showed large haplotype and small nucleotide diversities, departures from neutral expectations, and haplotype networks consistent with persistent genetic structuring of the species population. These patterns of diversity indicate the presence of selection driving population divergence. We hypothesize that position-keeping by this deep-living, non-migrating euphausiid species may prevent genetic homogenization (panmixia) in the dynamic Gulf Stream System. This study demonstrates the importance of analyzing patterns of genetic diversity and structure at regional and global scales to understand the ecological and evolutionary processes impacting marine zooplankton.

**Keywords:** COI barcode, euphausiid, Gulf Stream, phylogeography

## Introduction

### The genus *Stylocheiron*

The euphausiid genus *Stylocheiron* comprises 12 accepted species, many of which are widely distributed throughout temperate and tropical regions of the Atlantic, Pacific, and Indian oceans, according to the World Register of Marine Species (WoRMS Editorial Board, 2021). Our understanding of the systematic relationships of the *Stylocheiron* species has been guided by hypothesized patterns of evolution of eye shape and appendage morphology (Brinton *et al.*, 1999). The distinctive bilobed eye, small number of photophores, lack or reduction of the fourth-to-eighth thoracic appendages, and elongation of the third thoracic appendage are diagnostic characteristics of the genus *Stylocheiron* (Mauchline, 1980; Brinton *et al.*, 1999). These characteristics have been used to discriminate two groups of species within the genus, the

*Stylocheiron longicorne* group (consisting of seven species: *S. longicorne, Stylocheiron affine, Stylocheiron elongatum*, *Stylocheiron indicum, Stylocheiron insulare, Stylocheiron microphthalma*, and *Stylocheiron suhmii*) and the *Stylocheiron maximum* group (consisting of three species: *Stylocheiron abbreviatum*, *Stylocheiron robustum*, and *S. maximum*; Brinton, 1962; Brinton *et al.*, 1999). Multi-gene phylogenetic analysis has been used in tandem with morphological assessment to examine euphausiid diversity and evolution. Such integrative morphological molecular taxonomic analyses have yielded a consensus view of the species diversity and evolutionary history of euphausiids as a group (Bucklin *et al.*, 2007; Vereshchaka *et al.*, 2019), although significant questions remain.

Analysis of the mitochondrial cytochrome oxidase I (COI) barcode region has yielded useful insights into the diversity of euphausiids (Bucklin *et al.*, 2007), including species of *Stylocheiron* (Wiebe *et al.*, 2016). Two species of *Stylocheiron* exhibit unusual levels of morphological variation, apparently associated with variation in oceanographic conditions across their extensive geographic ranges spanning multiple ocean basins. Brinton (1962) distinguished five morphological variants (which he called "forms") of *S. affine* and two forms of *S. longicorne*. The geographic extent and disjunct distributions of the species have given rise to questions about the taxonomic significance of geographical variation in morphological characters. Examination of COI barcode variability of *S. affine* confirmed significant genetic differentiation among populations and suggested the presence of a cryptic species of *S. affine* in the Red Sea, for which COI barcode data showed divergence consistent with speciation (Wiebe *et al.*, 2016).

### *Stylocheiron elongatum*

*Stylocheiron elongatum* is one of the most geographically widespread species of the genus, with a latitudinal range of 60°N–40°S (Mauchline, 1980). The species occurs from 35°S to 65°N in the Atlantic Ocean, from 40°N to 35°S in the Pacific Ocean, and across the Indian Ocean north of 40°S (Brinton, 1962; WORMS Editorial Board, 2021). The species lives deeper than any other member of the *S. longicorne* species group, is classified as a mesopelagic species and shows little evidence of diel vertical migration behavior (Brinton *et al.*, 1999). The vertical distribution of *S. elongatum* was reported to be 300–500 m in the Gulf Stream, Gulf Stream rings, and Sargasso Sea (Wiebe and Flierl, 1983). Hydrographic conditions, including the presence of warm and cold core Gulf Stream rings were shown to impact the species' vertical distribution (Wiebe and Flierl, 1983; Endo and Wiebe, 2007).

### The Gulf Stream system

The Gulf Stream has been likened to a river in the sea; over much of its course, its strongest signature (in terms of temperature, salinity, and transport) is in the surface 100 m (Worthington, 1976). Transport in the Gulf Stream increases approximately fivefold from the initial concentration of flow of the Florida Current (FC), which flows from the Dry Tortugas to Nova Scotia; the increase results largely from the entrainment of Sargasso Sea waters and to a lesser degree shelf and Slope Water (Heiderich and Todd, 2020). Current velocities and transport volumes of the FC vary seasonally (Meunier *et al.*, 2018), resulting in variable concentrations and source regions of the entrained zooplankton (Davis and Wiebe, 1985).

The Gulf Stream Meander Region (GSMR) flows eastward from Cape Hatteras to the Grand Banks and beyond, and is characterized by a complex hydrography and circuitous path, with significant impacts on biological processes and productivity (Gaube and McGillicuddy, 2017). In this dynamic region, meanders develop and intensify, cold- and warm-core rings spin off to the south and north, respectively, and water from different domains is mixed into the flow (Meinen and Luther, 2016).

### Population genetic diversity and structure of zooplankton

Patterns of population genetic diversity and structure, also called phylogeography (Avise, 2000), can provide unique insights into the ecological, evolutionary, and taxonomic significance of geographic variation of marine zooplankton with widespread and disjunct distributions. COI and another mitochondrial protein-coding gene, cytochrome b (CYB), have been used to examine evolutionary processes within species of a wide range of animals (Kocher *et al.*, 1989; Tobe *et al.*, 2010). Several euphausiids with extensive biogeographical distributions have been examined for molecular genetic variation of COI and/or CYB, including *Meganyctiphanes norvegica* (Bucklin *et al.*, 1997; Patarnello *et al.*, 2010) and other species (Raupach and Radulovici, 2015; Kulagin *et al.*, 2021).

The population genetic consequences of the exceptionally large population sizes of marine organisms have been a topic of continuing interest (Waples, 2016). Peijnenburg and Goetze (2013) reviewed evidence that selection may be a dominant driver of the evolution of open-ocean zooplankton, including findings of non-neutral evolution, discrepancies between census and effective population sizes, and differences between unlinked genetic markers. A number of studies have examined the importance of selection for marine organisms (Sanford and Kelly, 2011; Plough, 2016), including purifying selection, which eliminates even slightly-disadvantageous mutations and may be especially effective in extremely large populations (Nei, 1987; Hughes, 2005). Although the distributions of most *Stylocheiron* species, including *S. elongatum,* span multiple ocean basins with typically highly abundant populations, genetic diversity is small and there is little or no genetic differentiation of geographic populations, based on available COI barcode data (Bucklin *et al.*, 2021; Figure 1). These global-scale patterns of COI barcode diversity of *Stylocheiron* species provide the context for our analysis of population structure and connectivity of *S. elongatum* in the NW Atlantic Ocean.

Regional scale studies of marine zooplankton, ideally using a variety of genetic markers, are important to examine patterns of diversity and structure in relation to ocean processes and to trace pathways of connectivity (Aarbakke *et al.*, 2014; Questel *et al.*, 2016). Such studies can also determine the temporal persistence of population genetic differentiation and structure (Avise, 2004; Peijnenburg and Goetze, 2013). This study examines haplotype and nucleotide diversities based on short regions of mitochondrial COI and CYB for *S. elongatum* samples collected in the NW Atlantic Ocean. Patterns of genetic diversity are examined for evidence of selection driving population divergence of *S. elongatum* along the Gulf Stream system. The results are used to test the hypothesis that deep-dwelling, non-migrating zooplankton may maintain persistent population isolation and genetic differentiation, even in dynamic current regimes (Harkins *et al.*, 2013; Goetze *et al.*, 2015).

## Material and methods

### COI barcodes of *Stylocheiron* species

DNA sequences for the COI barcode region were obtained for eight *Stylocheiron* species from the MetaZooGene Barcode Atlas

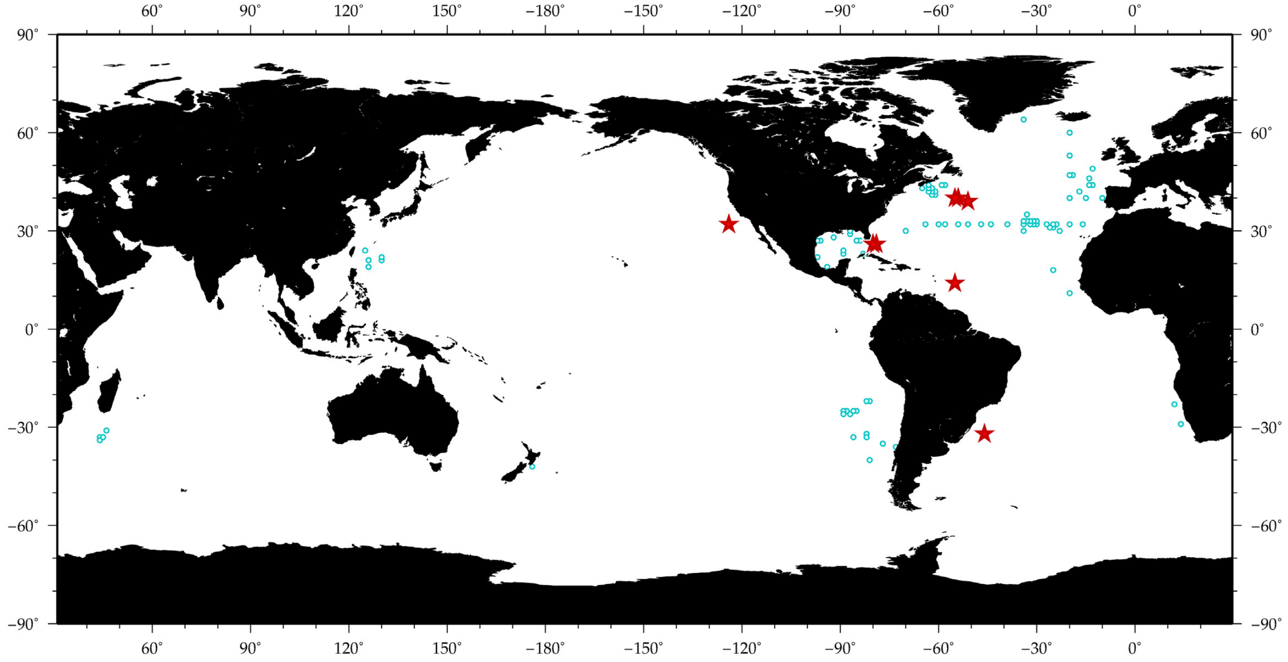

**Figure 1.** Distribution of *S. elongatum* based on collection records from the Coastal and Oceanic Plankton Ecology, Production, and Observation Database (COPEPOD, see https://www.st.nmfs.noaa.gov/copepod/) and barcoding records of the MetaZooGene Barcode Atlas and Database (see https://metazoogene.org/database). Collection locations are shown for identified specimens (blue dots) and specimens for which COI barcode data are publicly available (red stars). Figure accessed online via the MetaZooGene Atlas and Database (MZGdb; https://metazoogene.org/atlas).

and Database (MZGdb; https://metazoogene.org/database), a public repository of barcode data and metadata accessed from NCBI GenBank and BOLD (Bucklin *et al.*, 2021). All barcode records for *Stylocheiron* species that included collection metadata (latitude and longitude) were used for analysis (Figure 2; Supplementary Table S1). Some of the COI sequences were determined for this study from archived specimens of *Stylocheiron* species resulting from the Census of Marine Zooplankton program (see http://www.cmarz.org/). Protocols for DNA sequencing were as described in Bucklin *et al.* (2007). PCR amplification used the consensus primers, LCO-1490 [5"-GGTCAACAAATCATAAAGATATTGG-3"] and HCO-2198 [5"-TAAACTTCAGGGTGACCAAAAAATCA-3"] (Folmer *et al.*, 1994). Sequences were aligned using the Muscle algorithm (Edgar, 2004) and trimmed to a uniform length for analysis using Molecular Evolutionary Genetics Analysis (MEGA 7; Kumar *et al.*, 2016).

## Collection and preservation of zooplankton samples

Collections of zooplankton samples containing *S. elongatum* for this study were made during two research cruises in the N. Atlantic Ocean in 1993 (Table 1). The *R/V Calanus* (CA-9303; 28 February–3 March 1993) sampled a transect across the FC, including ten vertically-integrated, oblique tows of a 1-m$^2$ ring net (333 μm mesh) and five vertically-stratified casts of a 1-m$^2$ Multiple Opening and Closing Net and Environmental Sensing System (MOCNESS; Wiebe *et al.*, 1985). The *R/V Oceanus* (OCE-258; 18–27 April 1993) traversed the GSMR in the N. Atlantic Ocean, with collection of 25 zooplankton samples by integrated, oblique tows of a 1-m$^2$ ring net, hydrographic data, and Acoustic Doppler Current Profiles (ADCP) during six crossings of the Gulf Stream (see Bucklin *et al.*, 1996). During both cruises, zooplankton samples were preserved immediately in 95% ethyl alcohol; the alcohol was changed once 24 hrs after collection.

## Physical oceanographic measurements

Hydrographic information was collected during the MOCNESS tows at five locations across the FC during CA-9303 in February 1993. Vertical temperature structure was characterized based on Expendable BathyThermograph (XBT) profiles at the site of each 1-m$^2$ ring net tow during OCE-258. Hydrographic data were summarized by Bucklin *et al.* (1996). During the OCE-258 cruise in April 1993, the Gulf Stream, Slope Water, and Sargasso Sea were delimited based on the NOAA/NOS oceanographic features analysis of sea surface temperature (SST) obtained from satellite-based Advanced Very High Resolution Radiometry (AVHRR). The ship's position was plotted on charts obtained from NOAA daily during the cruise, and sampling strategies were determined in part from this information. A spatially complete SST map for 23 April 1993 was produced by interpolation to fill in gaps based on NOAA 1/4° daily Optimum Interpolation Sea Surface Temperature (OISST), which combines observations from different platforms (satellites, ships, buoys) on a regular global grid (Figure 3).

## Genetic analysis of *S. elongatum*

Individuals of *S. elongatum* for genetic analysis were removed from FC and GSMR samples, with taxonomic identification confirmed using diagnostic microscopic morphological characteristics (Brinton, 1962). A total of 94 individuals of *S. elongatum* were identified: 54 from FC and 40 from GSMR samples, although not all

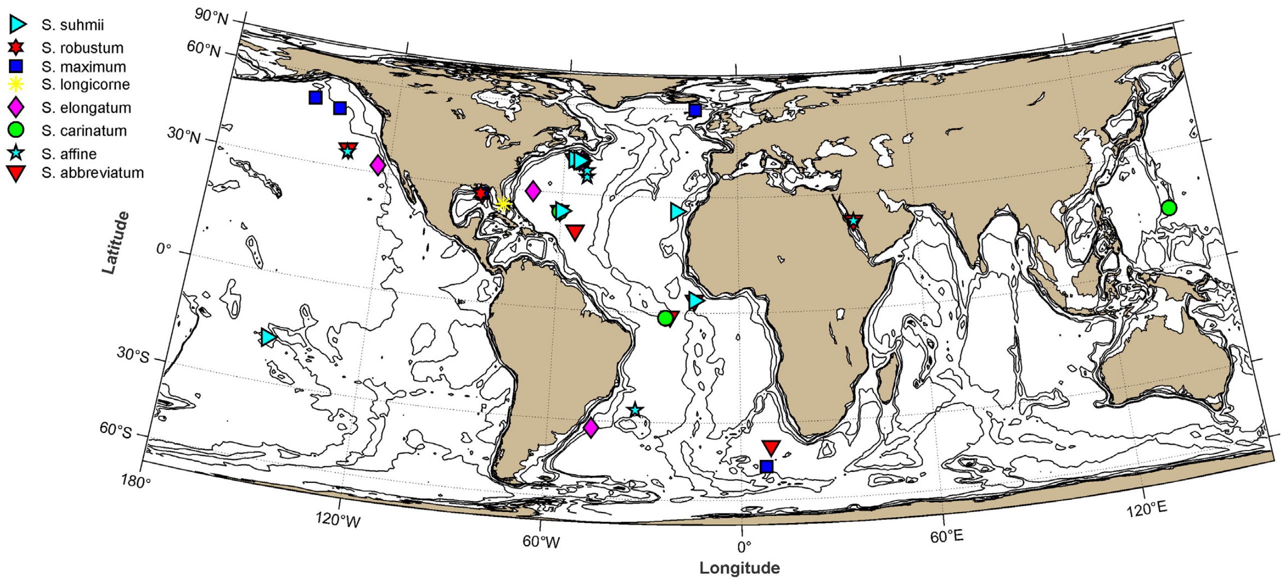

**Figure 2.** Map of collection locations of identified specimens of *Stylocheiron* species from which COI barcode data were analyzed for this study. Data were accessed via the MetaZooGene Barcode Atlas and Database (MZGdb; https://metazoogene.org/database).

**Table 1.** Collection information for *S. elongatum* samples from the FC (CA-9303; 28 February–3 March 1993) and from the GSMR (OCE-258; 18–27 April 1993) used for genetic analysis in this study. Collection times are given in local time. Depths are given as estimated for integrated tows; maximum sampling depths are provided for each sample collection. Numbers of individuals (*N*) of *S. elongatum* collected and identified from each sample are given, but not all individuals were sequenced for both genes regions.

| **R/V *Calanus* (CA9303; 28 February–3 March, 1993)** | | | | | |
|---|---|---|---|---|---|
| **Sta. #** | **Date** | **Time** | **Latitude; Longitude** | **Max depth (m)** | ***N*** |
| MFL-001 | 22-Feb-93 | 14:25 | 25°45.1“ N 79°40.0” W | 400 | 8 |
| MFL-002 | 22-Feb-93 | 16:55 | 25°44.9“ N 79°44.0” W | 540 | 5 |
| MFL-003 | 23-Feb-93 | 0:25 | 25°44.9“ N 79°25.4” W | 520 | 10 |
| MFL-004 | 23-Feb-93 | 0:00 | 25°44.9“ N 79°31.1” W | 450 | 3 |
| MFL-005 | 24-Feb-93 | 0:00 | 25°45.3“ N 79°39.1”W | 450 | 10 |
| M2 | 22-Feb-93 | 21:30 | 25°45.0“ N 79°46.3” W | 300 | 14 |
| M3 | 22-Feb-93 | 22:22 | 25°45.0“ N 79°47.4” W | 300 | 4 |
| Total | | | | | 54 |
| **R/V *Oceanus* (OCE-258; 18–27 April, 1993)** | | | | | |
| **Sta. #** | **Date** | **Time** | **Latitude; Longitude** | **Max depth** (m) | ***N*** |
| OCE-14 | 21-Apr-03 | 6:52 | 39°46.3“ N 54°44.7” W | 400 | 9 |
| OCE-17 | 22-Apr-03 | 10:15 | 39°42.1“ N 54°05.4” W | 400 | 1 |
| OCE-18 | 22-Apr-03 | 11:38 | 39°41.5“ N 54°00.0” W | 400 | 14 |
| OCE-19 | 22-Apr-03 | 13:03 | 39°41.0“ N 53°54.0” W | 400 | 12 |
| OCE-20 | 23-Apr-03 | 3:10 | 39°25.9“ N 50°33.7” W | 400 | 4 |
| Total | | | | | 40 |

yielded sequences for analysis (Table 1; Supplementary Table S2). All specimens of the target species were removed from the analyzed samples, with the exception of small individuals. DNA was purified from identified specimens of *S. elongatum* by phenol extraction and ethanol precipitation using protocols previously used for barcoding euphausiids (Bucklin, 2000; Bucklin *et al.*, 2007). The purified DNA was used to amplify two regions of mitochondrial DNA: COI and CYB. The COI region analyzed differed from the usual barcode region (Folmer *et al.*, 1994) and was amplified using the consensus primer, (COI-f [5'—CCTGCAGGAGGAGGAGATCC–3“] (Palumbi, 1996) and a euphausiid-specific primer designed for this study, COI-609 [5”—GACGAGGTATTCCATTTAATC–3“]. The CYB protocol used PCR primers: CYB-L14841 [5”—CCATCCAACATCTCAGCATGATGAAA–3“] and CYB-H15149 [5”—CCCTCAGAATGATATTTGTCCTCA–3'] (Kocher *et al.*, 1989). The PCR protocol for both COI and CYB was: 94°C (1 min); 42°C (2 min); and 72°C (3 min) for 40 cycles. The COI-f and CYB-1 primers were used for sequencing; complementary reactions using CYB-2 were done for some individuals in order to verify substitutions at particular sites. All sequences were manually checked for accuracy, including viewing of chromatogram files, prior to analysis using MEGA 7 (Kumar *et al.*, 2016).

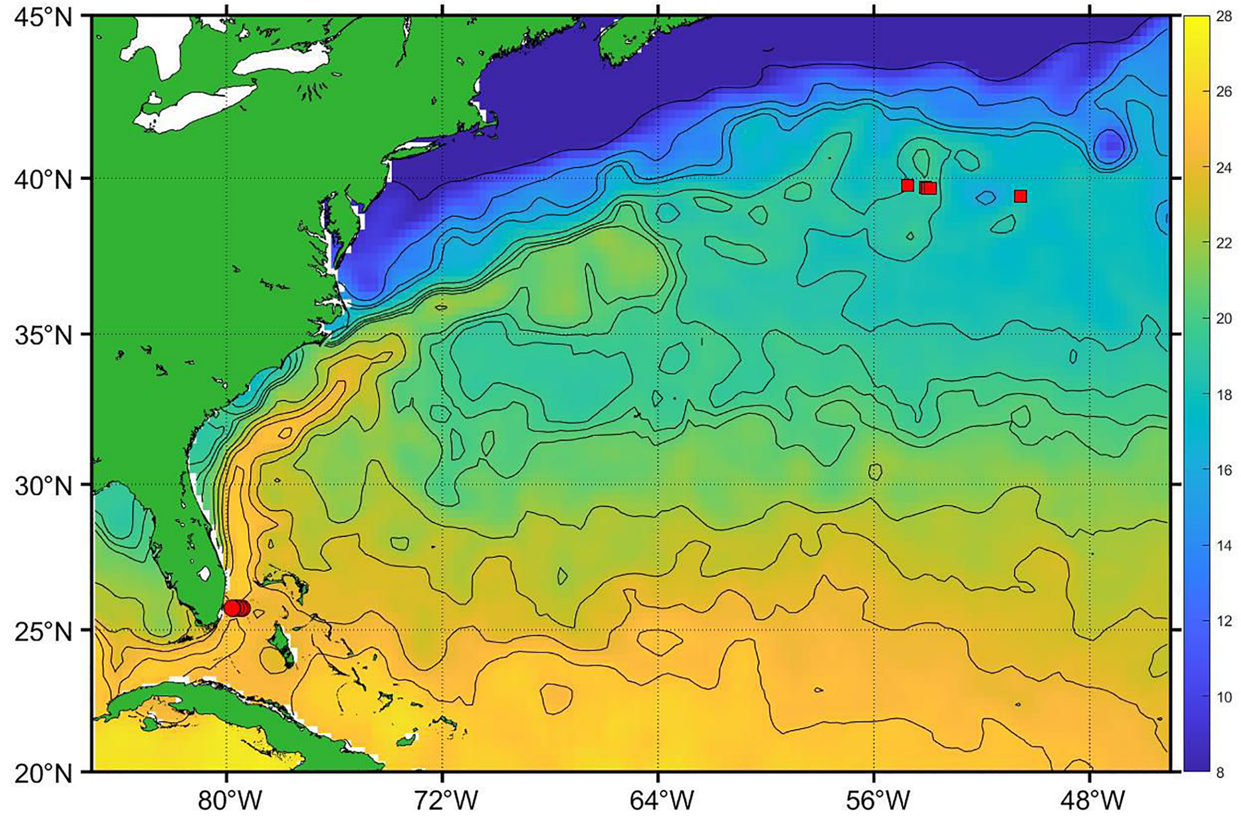

**Figure 3.** Collection locations of *S. elongatum* analyzed in this study with overlay of SST based on AVHRR data for 23 April 1993. The outlines show currents and water mass features in the western N. Atlantic Ocean, including the Gulf Stream, meanders, rings, and entrainment features. AVHRR data downloaded from National Oceanic and Atmospheric Administration (NOAA; see https://www.ncdc.noaa.gov/oisst/data-access). Sample collection location coordinates are provided in Table 1.

## Population genetic and phylogeographic analysis of *S. elongatum*

Population genetic diversity and structure of *S. elongatum* were evaluated based on DNA sequence variation of both mitochondrial COI and CYB gene regions. Confirmation of species identification as *S. elongatum* was based on BLAST searches of the NCBI GenBank database (Altschul *et al.*, 1997) and matches to *S. elongatum* records with $E = 0$, where E is the expected number of matches by chance. Sequences for each gene region were aligned using the Muscle algorithm (Edgar, 2004) and trimmed for analysis using MEGA 7. Analysis was based on sequence alignments for 82 individuals for a 394 base-pair (bp) region of COI; for 84 individuals for a 308 bp region of CYB; and for 68 individuals for a 702 bp for COI + CYB (Supplementary Table S2).

Nucleotide ($\theta_\pi$) and haplotype ($h_d$) diversity for the COI, CYB, and COI + CYB gene regions were estimated using DnaSP 5 (Librado and Rozas, 2009). Neutrality was tested with Tajima's *D* (Tajima, 1989) using DnaSP 6 (Rozas *et al.*, 2017). The best-fitting substitution model, Tamura 92 (Tamura, 1992), was selected with MEGA 7, using the Akaike information criterion (Kumar *et al.*, 2016). A hierarchical Analysis of MOlecular VAriance (AMOVA) with the Tamura (1992) mutation model was used to examine population genetic structure using Arlequin 3.5 (Excoffier and Lischer, 2010). Samples were grouped by geographic region (FC vs. GSMR; Table 1). Variance partitions were tested for significance under 10 100 permutations, with $\alpha = 0.05$, after sequential Bonferroni correction (Holm, 1979). Negative $\Phi_{ST}$ values were assumed to be zero. Haplotype networks were estimated using Haploviewer (Center for Integrative Bioinformatics; available at http://www.cibiv.at/~greg/haploviewer).

Gene flow between regions for *S. elongatum* was modeled using the coalescent-based program Migrate-N 4.4.3 (Beerli, 2016). Migrate-N uses ratios of maximum likelihood, or Bayesian inference to estimate migration rates and effective population size ($N_E$) under the assumption of asymmetrical migration rates at different subpopulation sizes (Beerli and Felsenstein, 2001). Four model scenarios were tested for each marker using Migrate-N: Full model, allowing for unrestricted gene flow between all sampled locations; FC-to-GSMR, allowing only northward gene flow; GSMR-to-FC, allowing only southward gene flow; and Panmictic, with all samples treated as a single population. Migrate-N parameter settings for theta ($\theta$), migration rates ($M$), and Markov long–chain values were determined for optimal posterior distributions from initial $F_{ST}$-based runs using the Metropolis-Hastings sampling method (Hastings, 1970). Bayesian factor predictions for the four model scenarios are reported.

## Analysis of COI barcode variation of *Stylocheiron* species

Sequence variation of the COI barcode region was evaluated within and between species of *Stylocheiron* by calculating the average and standard deviation of pairwise proportional nucleotide distance

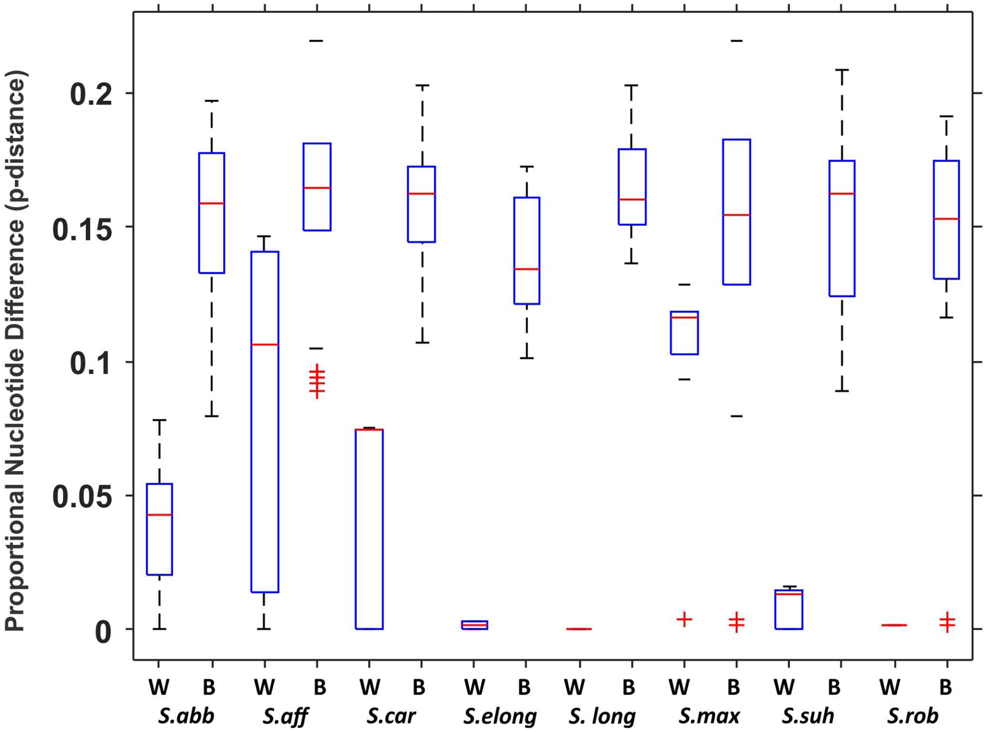

**Figure 4.** COI barcode proportional pairwise differences (p-distances) within (W) and between (B) eight species of *Stylocheiron*. Results reflect pairwise comparisons between COI sequences for 64 specimens of eight species (see Supplementary Tables S1 and S3). Box plot shows: 25 and 75 percentile range (blue boxes); 50 percentile (red lines); 5 and 95 percentile limits (dashed lines); and outliers (red crosses).

(p-distance) between individual specimens of the same and different species. A COI gene tree was constructed using MEGA 7 (Kumar *et al.*, 2016) with the Neighbor Joining algorithm (Saitou and Nei, 1987), Tamura (1992) distances, and 1000 bootstraps.

## Results

### COI barcode variation among *Stylocheiron* species

DNA sequences for a 498 bp section of the usual barcode region of COI (Folmer *et al.*, 1994) showed pairwise differences averaging 14–16% between individuals of different species of *Stylocheiron* examined in this study (Figure 4 and Supplementary Table S3). This range is consistent with interspecific differences observed in previous studies of euphausiids, including *Stylocheiron* (Bucklin *et al.*, 2007; Wiebe *et al.*, 2016). Intraspecific variation was very low for several species, including *S. elongatum*, which showed $<$ 1% differences among four specimens collected in different ocean basins, and *S. longicorne* and *S. robustum*, for which low levels of intraspecific COI variation were likely due to small sample sizes (Figure 4 and Supplementary Table S3). Intraspecific COI variation was markedly greater for *S. affine*, which may reflect possible cryptic speciation (Wiebe *et al.*, 2016). Uncertain species identification may cause higher intraspecific variation for *S. maximum* (Bucklin *et al.*, 2007).

The Neighbor-Joining COI gene tree resolved most species of *Stylocheiron* with high boostrap support (Figure 5). Although barcodes for *S. abbreviatum* clustered with 99% bootstrap support, there was no clear resolution of geographic variation across multiple ocean basins (Figure 5). Barcodes for *S. robustum* from the Gulf of Mexico (Wilkins and Bracken-Grissom, unpublished data) were intermixed with *S. maximum*. A total of three of the four "longicorne" group species (Brinton *et al.*, 1999) were included in a single cluster with 93% bootstrap value; within the cluster, *S. longicorne* and *S. suhmii* had 100% bootstrap values, but *S. affine* showed significant divergence of Red Sea samples from those of Atlantic and Pacific oceans (Figure 5), representing a possible cryptic species (Wiebe *et al.*, 2016).

### Collection of *S. elongatum*

A total of 94 individuals of *S. elongatum* were identified from samples collected in the NW Atlantic: 54 from FC and 40 from GSMR samples, although not all yielded sequences for analysis (Supplementary Table S2). Vertical distributions of *S. elongatum* analyzed from FC were between 200 and 300 m in the daytime and between 200 and 350 m during nighttime, based on MOCNESS deployments (Table 1). Temperature profiles collected across the FC showed the vertical distribution of *S. elongatum* centered between the 13 and 17°C contours in both day- and night-time MOCNESS tows (see Bucklin *et al.*, 1996).

### Variation of COI and CYB of *S. elongatum*

Haplotype diversity of the sampled individuals of *S. elongatum* was larger for the 394 bp region of COI, with 37 haplotypes among 83 individuals ($h_d = 0.902 \pm 0.022$) than for the 308 bp region of CYB, with 21 haplotypes among 84 individuals ($h_d = 0.474 \pm 0.069$); COI + CYB values reflected the COI levels, with 42 haplotypes among 68 individuals ($h_d = 0.920 \pm 0.025$; Table 2). Nucleotide diversity showed similar patterns, with COI significantly more variable ($\theta_\pi = 0.0096 \pm 0.001$) than CYB ($\theta_\pi = 0.0035 \pm 0.001$) or

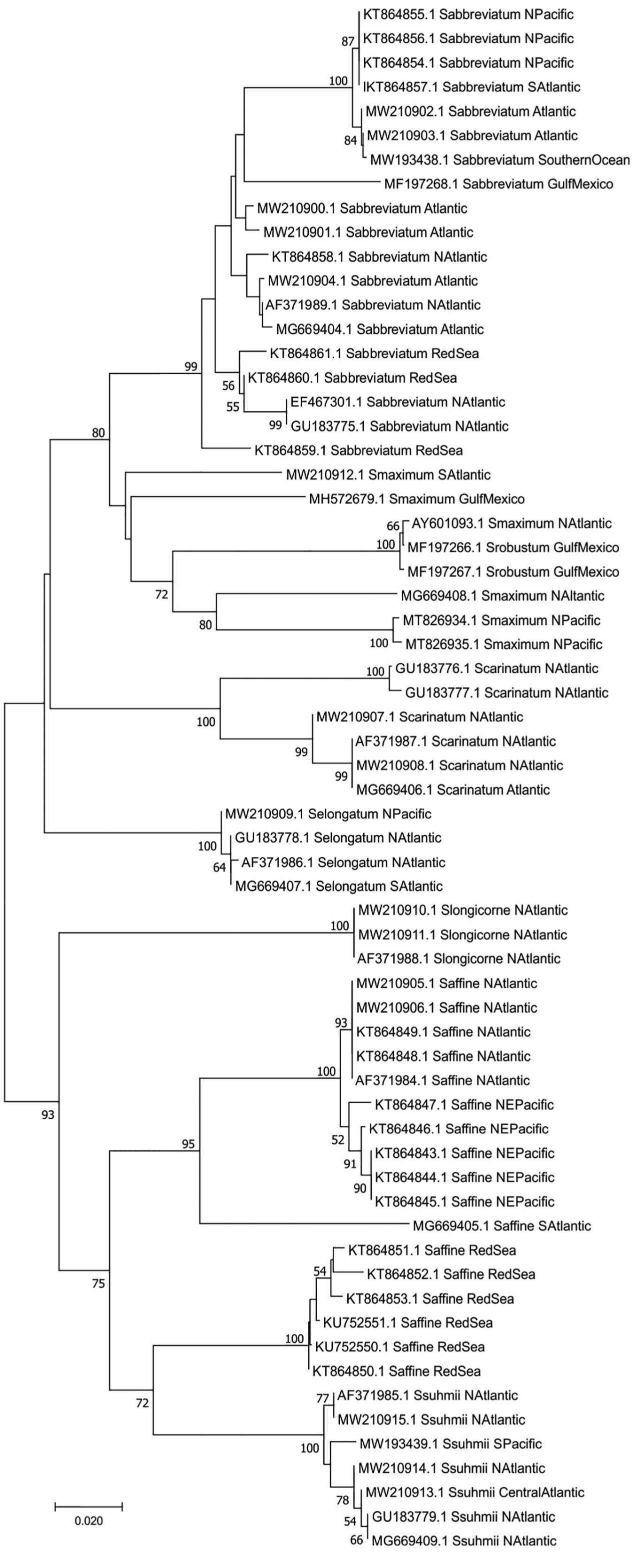

**Figure 5.** COI barcode gene tree for *Stylocheiron* species based on sequences available in the MetaZooGene Barcoding Atlas and Database (see https://metazoogene.org/database). Neighbor Joining tree with Tamura (1992) substitution model; 1000× bootstrap values are indicated at nodes; values > 50 are shown. See Supplementary Table S1 for collection metadata and citations for sources of sequences. See Figure 2 for map of collection locations by species.

COI + CYB ($\theta_\pi = 0.007 \pm 0.001$; Table 3). Analyses of all gene regions (COI, CYB, and COI + CYB) showed significant departures from neutral expectations (Librado and Rozas, 2009) based on Tajima's *D* (Tajima, 1989), estimated for the whole sequenced region and for polymorphic sites with synonymous, non-synonymous, and silent substitutions (Table 3).

Variance partitions ($\Phi_{ST}$) based on COI and COI + CYB were statistically significant for six pairwise comparisons between FC and GSMR samples, but only one comparison for CYB (Table 4). Population genetic structure analysis based on AMOVA (Excoffier and Lischer, 2010) analysis of COI + CYB showed significant differentiation between the two regions ($\Phi_{CT} = 0.066$, $p < 0.01$), among samples within regions ($\Phi_{SC} = 0.170$, $p < 0.001$), and within samples ($\Phi_{ST} = 0.225$, $p < 0.0001$; Table 5). CYB showed no significant variance partitions, and COI was significant for within and among samples, but not among regions (Table 5).

Haplotype networks showed two COI haplotypes that were most frequent in each of the two sampled regions of the Gulf Stream (FC and GSMR), with numerous additional haplotypes, most of which were unique to FC (Figure 6a). CYB showed a highly skewed haplotype frequency distribution, with a single dominant haplotype found in all samples, with four rarer shared haplotypes, and a number of unique haplotypes found mostly in FC (Figure 6b). For COI + CYB, the predominance of unique haplotypes restricted to FC was notable, with the two most frequent haplotypes occurring either exclusively (FC) or primarily (GSMR) in one region (Figure 6c).

Of the four model scenarios tested for each marker using Migrate-N (Beerli, 2016), the FC-to-GSMR model, with only northward gene flow, was the highest likelihood based on CYB and COI + CYB; probability was highest for COI for the Full model, i.e. bidirectional pairwise exchange among all samples (Table 6).

## Discussion

### Variation within and among species of *Stylocheiron* based on the COI barcode region

Patterns of DNA sequence variation of the COI barcode region within and among species of *Stylocheiron* (Figure 4, Supplementary Table S3) were similar to those among species of other euphausiids, including sibling and congeneric species, sequenced for this gene portion (Bucklin *et al.*, 2007; Wiebe *et al.*, 2016). Phylogenetic relationships among higher taxonomic groups are not usually resolved by the COI barcode region, but the gene tree did support some aspects of the species groupings described based on morphological characters (Brinton *et al.*, 1999), including significant (93% bootstrap) clustering of three of four barcoded species of the *S. longicorne* group (*S. longicorne, S. affine, S. suhmii*; but not *S. elongatum*); all three species of the *S. abbreviatum* group (*S. abbreviatum, S. maximum, and S. robustum*) were clustered with 80% bootstrap support (Figure 5).

The COI barcode has been widely used to identify potential cryptic species of marine zooplankton for which diagnostic taxonomic characters can be subtle or missing (Bucklin *et al.*, 2011; Peijnenburg and Goetze, 2013), including euphausiids (Bucklin *et al.*, 2007; Wiebe *et al.*, 2016). For the *Stylocheiron* species analyzed here, despite significant intraspecific variation associated with broad geographic distributions, the COI barcode provided reliable discrimination of species, usually with 100% bootstrap values (Figure 5). One species, *S. abbreviatum*, showed evidence of high levels of

**Table 2.** Summary of intraspecific variation of designated regions of COI and CYB for *S. elongatum*. $N$ = number of sequences; $BP$ = base pair sequence length; $h$ = number of haplotypes; $h_d$ = haplotype diversity, $\theta_\pi$ = nucleotide diversity, $SD$ = standard deviation.

| **Barcode** | ***N*** | ***BP*** | ***h*** | **$h_d$** | ***SD*** | $\theta_\pi$ | ***SD*** |
|---|---|---|---|---|---|---|---|
| COI | 83 | 394 | 37 | 0.902 | 0.022 | 0.010 | 0.001 |
| CYB | 84 | 308 | 21 | 0.474 | 0.069 | 0.003 | 0.001 |
| COI + CYB | 68 | 702 | 42 | 0.920 | 0.025 | 0.007 | 0.000 |

**Table 3.** Tajima's *D* values for COI and CYB variation of *S. elongatum*, for the entire analyzed sequence (All gene) and for synonymous, non-synonymous and silent polymorphic sites. Numbers of sites within each category are indicated by n; asterisks indicate significance levels ($^{*}$ $p < 0.05$, $^{**}$ $p < 0.01$, and $^{***}$ $p < 0.001$).

| **Barcode** | **All gene** | **Synonymous** | **Non-synonymous** | **Silent** |
|---|---|---|---|---|
| **COI** | $-2.402^{**}$ | $-1.893^{*}$ ($n = 16$) | $-2.450^{**}$ ($n = 28$) | $-1.893^{*}$ ($n = 16$) |
| **CYB** | $-2.561^{***}$ | $-1.831^{*}$ ($n = 5$) | $-2.497^{**}$ ($n = 21$) | $-1.831^{*}$ ($n = 5$) |

**Table 4.** Pairwise $\Phi_{ST}$ distances between samples of *S. elongatum* from the FC and GSMR. The mutation model used was the Tamura distance (Tamura, 1992) based on 10 100 permutations. $\Phi_{ST}$ values are below and $p$ values are above the diagonal. Negative values are shown as 0.000; bold values indicate significant values after sequential Bonferoni correction ($\alpha = 0.05$). See Table 1 for collection information and text for explanation of methods.

| | **Florida Current** | | | | | | **Gulf Stream** | | | | |
|---|---|---|---|---|---|---|---|---|---|---|---|
| **COI** | **MLF001** | **MLF002** | **MLF003** | **MLF005** | **M2** | **M3** | **14** | **18** | **19** | **20** | |
| MLF001 | | 0.496 | **0.001** | 0.117 | 0.156 | 1.000 | 0.158 | 0.006 | 0.003 | 0.115 | |
| MLF002 | **0.001** | | **0.001** | 0.778 | 0.086 | 1.000 | 0.016 | 0.013 | 0.002 | 0.020 | |
| MLF003 | **0.316** | **0.293** | | **0.001** | **0.001** | 1.000 | **0.001** | **0.001** | **0.000** | 0.049 | |
| MLF005 | 0.052 | **0.000** | **0.323** | | **0.001** | 1.000 | **0.001** | **0.001** | **0.000** | 0.031 | |
| M2 | 0.038 | 0.089 | 0.217 | 0.141 | | 1.000 | 0.140 | 0.276 | 0.015 | 0.529 | |
| M3 | 0.752 | 1.000 | 0.326 | 0.819 | 0.554 | | 0.144 | 0.072 | 0.090 | 0.252 | |
| 14 | 0.076 | 0.266 | **0.322** | **0.288** | 0.051 | 0.672 | | 0.040 | 0.110 | 0.879 | |
| 18 | 0.160 | 0.242 | **0.250** | **0.229** | 0.016 | 0.747 | 0.129 | | 0.019 | 1.000 | |
| 19 | 0.249 | 0.648 | **0.448** | **0.409** | 0.103 | 0.942 | 0.138 | 0.139 | | 0.556 | |
| 20 | 0.135 | 1.000 | 0.282 | 0.356 | 0.000 | 1.000 | 0.000 | 0.000 | 0.008 | | |
| **CYB** | MLF001 | MLF002 | MLF003 | MLF005 | M2 | M3 | 14 | 17 | 18 | 19 | 20 |
| MLF001 | | 0.623 | 0.004 | 0.044 | 0.159 | 0.330 | 0.007 | 1.000 | 0.030 | **0.001** | 0.618 |
| MLF002 | 0.000 | | 1.000 | 1.000 | 1.000 | 0.426 | 0.515 | 1.000 | 1.000 | 1.000 | 1.000 |
| MLF003 | 0.085 | 0.000 | | 0.353 | 0.712 | 0.325 | 0.129 | 1.000 | 0.109 | 0.198 | 1.000 |
| MLF005 | 0.081 | 0.000 | 0.015 | | 0.552 | 0.253 | 0.211 | 1.000 | 0.667 | 0.176 | 1.000 |
| M2 | 0.040 | 0.000 | 0.000 | 0.000 | | 0.302 | 1.000 | 0.925 | 0.743 | 1.000 | 0.468 |
| M3 | 0.042 | 0.111 | 0.088 | 0.189 | 0.000 | | 0.679 | 1.000 | 0.225 | 0.204 | 0.420 |
| 14 | 0.106 | 0.000 | 0.062 | 0.080 | 0.009 | 0.000 | | 1.000 | 0.150 | 0.154 | 0.516 |
| 17 | 0.000 | 0.000 | 0.000 | 0.000 | 0.000 | 0.000 | 0.000 | | 1.000 | 1.000 | 1.000 |
| 18 | 0.071 | 0.000 | 0.022 | 0.000 | 0.000 | 0.137 | 0.049 | 0.000 | | 0.779 | 1.000 |
| 19 | **0.162** | 0.000 | 0.021 | 0.019 | 0.000 | 0.360 | 0.118 | 0.000 | 0.000 | | 1.000 |
| 20 | 0.000 | 0.000 | 0.000 | 0.000 | 0.000 | 0.000 | 0.000 | 0.000 | 0.000 | 0.000 | |
| **COI + CYB** | MLF001 | MLF002 | MLF003 | MLF005 | M2 | M3 | 14 | 18 | 19 | 20 | |
| MLF001 | | 0.087 | **0.001** | 0.029 | 0.352 | 0.120 | 0.254 | 0.052 | **0.001** | 0.350 | |
| MLF002 | 0.136 | | 0.004 | 0.219 | 0.101 | 0.200 | 0.083 | 0.002 | **0.001** | 0.029 | |
| MLF003 | **0.252** | 0.308 | | **0.000** | **0.000** | 0.218 | **0.001** | **0.001** | **0.000** | 0.061 | |
| MLF005 | 0.079 | 0.071 | **0.327** | | 0.007 | 0.096 | 0.011 | 0.001 | **0.000** | 0.004 | |
| M2 | 0.006 | 0.099 | **0.192** | 0.100 | | 1.000 | 0.622 | 0.315 | 0.015 | 0.612 | |
| M3 | 0.502 | 1.000 | 0.216 | 0.795 | 0.381 | | 1.000 | 1.000 | 1.000 | 1.000 | |
| 14 | 0.022 | 0.267 | **0.262** | 0.182 | 0.000 | 0.675 | | 0.634 | 0.075 | 0.646 | |
| 18 | 0.056 | 0.339 | **0.311** | 0.204 | 0.012 | 0.700 | 0.000 | | 0.133 | 0.921 | |
| 19 | **0.187** | **0.731** | **0.413** | **0.396** | 0.077 | 0.922 | 0.095 | 0.027 | | 1.000 | |
| 20 | 0.012 | 1.000 | 0.233 | 0.349 | 0.000 | 1.000 | 0.000 | 0.000 | 0.000 | | |

**Table 5.** Analysis of MOlecular VAriance (AMOVA) for *S. elongatum* collected from two regions, FC and GSMR. Fixation indices are shown for among regions ($\Phi_{CT}$), among samples within regions ($\Phi_{SC}$), and within samples ($\Phi_{ST}$). Calculations used the Tamura (1992) substitution model. Values shown in bold font indicate statistical significance ($p < 0.05$). *DF* = degrees of freedom.

| Barcode source of variation | *DF* | Sum of squares | Variance components | Percent of variation | Fixation indices | *p* value |
|---|---|---|---|---|---|---|
| **COI** | | | | | | |
| Among regions | 1 | 9.15 | 0.0847 | 4.21 | $\Phi_{CT} = 0.042$ | 0.074 ± 0.003 |
| Among samples, within regions | 8 | 37.64 | 0.4132 | 20.54 | **$\Phi_{SC} = 0.215$** | **< 0.001** |
| Within samples | 73 | 110.48 | 1.5134 | 75.24 | **$\Phi_{ST} = 0.248$** | **< 0.001** |
| Total | 82 | 157.27 | 2.0114 | | | |
| **CYB** | | | | | | |
| Among regions | 1 | 0.58 | −0.0027 | −0.42 | $\Phi_{CT} = -0.004$ | 0.745 ± 0.004 |
| Among samples, within regions | 9 | 6.12 | 0.0055 | 0.86 | $\Phi_{SC} = 0.009$ | 0.323 ± 0.004 |
| Within samples | 73 | 46.80 | 0.6410 | 99.56 | $\Phi_{ST} = 0.004$ | 0.331 ± 0.005 |
| Total | 83 | 53.50 | 0.6439 | | | |
| **COI + CYB** | | | | | | |
| Among regions | 1 | 12.03 | 0.1858 | 5.59 | **$\Phi_{CT} = 0.066$** | **0.009 ± 0.001** |
| Among samples, within regions | 8 | 40.46 | 0.4475 | 15.87 | **$\Phi_{SC} = 0.170$** | **< 0.001** |
| Within samples | 58 | 126.82 | 2.1865 | 77.54 | **$\Phi_{ST} = 0.225$** | **< 0.001** |
| Total | 67 | 179.31 | 2.8199 | | | |

genetic variation among samples collected throughout the species' geographical range, but without clear distinctions among oceanic regions; one clearly defined clade (100% bootstrap) included samples from the S Atlantic and NE Pacific, and another less well-resolved cluster included samples from the N Atlantic and Red Sea (Figure 5). In contrast, specimens of *S. affine* collected from the Red Sea showed clear genetic divergence based on the COI barcode from *S. affine* collected from the Atlantic and Pacific (Wiebe *et al.*, 2016; Figure 5). The Red Sea population of *S. affine* may represent a cryptic species (Wiebe *et al.*, 2016) and warrants further integrative morphological and molecular taxonomic analysis.

COI barcodes did not clearly discriminate two species, *S. maximum* and *S. robustum*, based on two sequences for *S. robustum* from the Gulf of Mexico available in NCBI GenBank (Wilkins and Bracken-Grissom, unpublished data). Morphological characteristics discriminating the species are subtle, and misidentification is always a concern. Analysis of additional samples and use of additional molecular markers, including population genomics approaches (Bucklin *et al.*, 2018), will be essential to ascertain the taxonomic and systematic relationships of the species.

## Population genetic diversity and structure of *S. elongatum*

The characterization of genetic diversity observed for *S. elongatum*, combining small nucleotide and large haplotype diversities, has been noted for marine zooplankton in previous studies (e.g. Peijnenburg and Goetze, 2013). Based on sequence variation of both COI and CYB, levels of $\theta_\pi$ were small and levels of $h_d$ were large for *S. elongatum*. Diversity was larger for COI ($\theta_\pi = 0.010$; $h_d = 0.902$) than for CYB ($\theta_\pi = 0.004$; $h_d = 0.474$; Table 2). Both gene regions showed significant departures from neutral expectations based on estimates of Tajima's D (Tajima, 1989), with non-synonymous sites showing more significant departures than synonymous sites (Table 3). Despite low levels of nucleotide diversity, patterns of variation of COI and COI + CYB revealed significant differences within and among samples within regions (Table 4); COI + CYB also showed significant differentiation between FC and GSMR regions (Table 5). The haplotype network for COI, with different haplotypes predominating in each region and unique and divergent haplotypes in FC (Figure 6a), is typical of populations that have been stable over evolutionary time.

The observed patterns of genetic diversity of *S. elongatum* in the NW Atlantic Ocean are consistent with the hypothesis of persistent genetic structuring (Avise, 2004). In particular, the departures from neutral expectations suggest the underlying driver of selection (Sanford and Kelly, 2011). We hypothesize that population divergence of *S. elongatum* results from the deeper distribution and lack of vertical migration behavior of the species, which may be expected to reduce rapid advection and slow transport by entrainment in the slower and less coherent current flow deeper in the Gulf Stream (Worthington, 1976).

The impacts of vertical distribution and migration behavior on population structure have been observed for zooplankton in diverse current systems (Miyamoto *et al.*, 2012; Harkins *et al.*, 2013; Goetze *et al.*, 2015). In contrast to *S. elongatum*, the copepod, *Nannocalanus minor*, showed genetic panmixia based on population genetic analysis by Bucklin *et al.* (1996), using samples collected during the same cruises (CA-9303 and OCE-258). Both species are distributed across the mid-latitudes of the N. Atlantic and are reproductive throughout the Caribbean source waters, FC, and GSMR (Wishner and Allison, 1986; Wiebe *et al.*, 1992). Neither species is thought to undergo marked diel vertical migration, but *N. minor* is an epipelagic species that is restricted to near-surface waters (Wishner and Allison, 1986), and populations of this species may be expected to be advected rapidly along the course of the Gulf Stream. Comparison of population genetic results for *N. minor* and *S. elongatum* is consistent with the hypothesis that advective transport in the Gulf Stream System is less effective in genetically homogenizing deeper-dwelling zooplankton species.

The population genetic diversity of *S. elongatum* may be compared with that of another euphausiid, *Meganyctiphanes norvegica*, for which the same mitochondrial COI and CYB gene regions were sequenced (Bucklin *et al.*, 1997). The two species have different geographical distributions, life histories, and behaviors: *M. norvegica* is a predominant member of the N. Atlantic zooplankton assemblage, with a distribution tied to the continental shelf, and exhibits

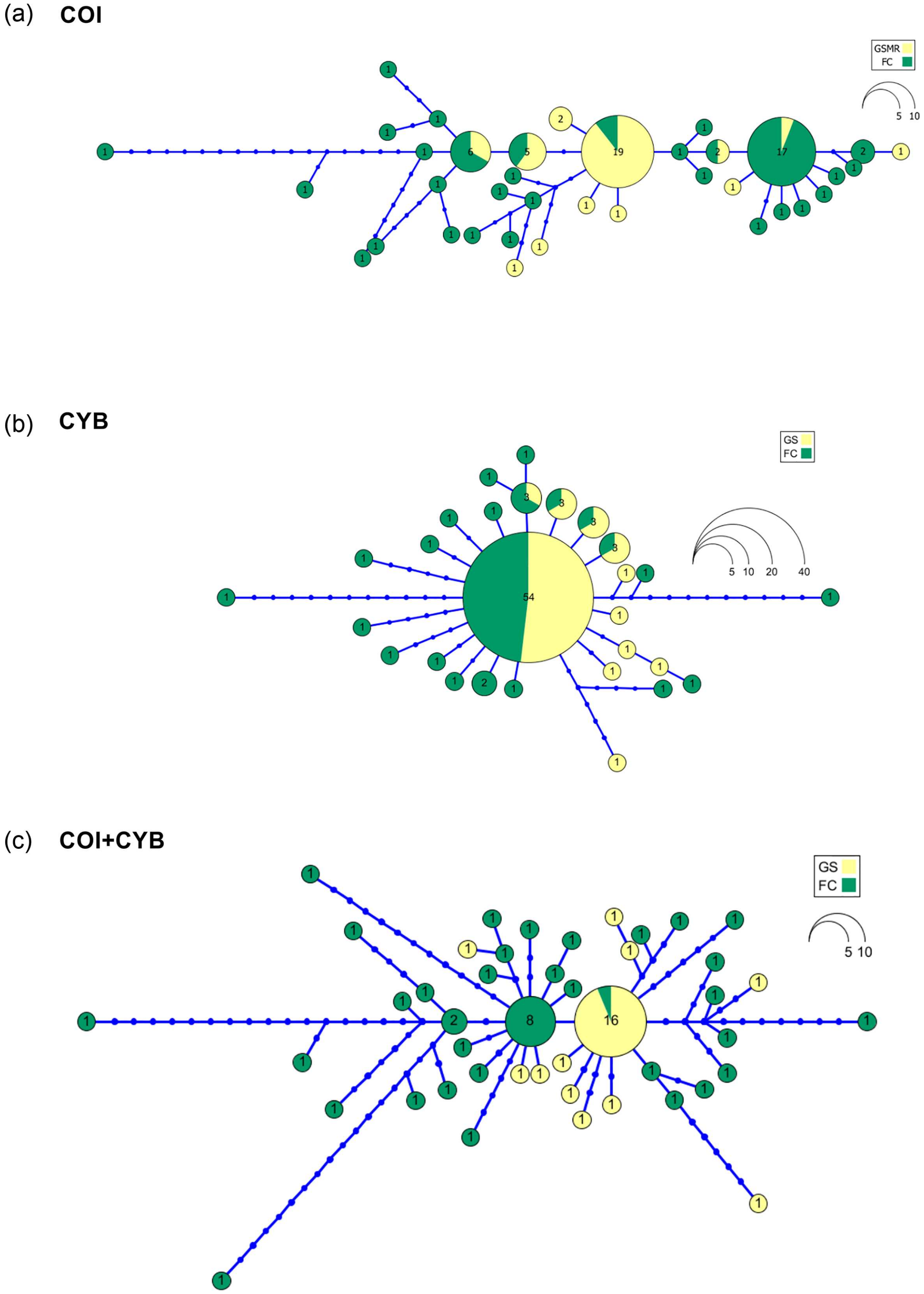

(a) COI

(b) CYB

(c) COI+CYB

**Figure 6.** Haplotype network diagrams for (a) COI, (b) CYB, and (c) COI + CYB for *S. elongatum*. Diagrams show numbers of individuals with each haplotype; cross-bars indicate numbers of substitutions separating haplotypes. Colors indicate collection region: Gulf Stream Meander Region (GSMR, yellow) and Florida Current (FC, green).

**Table 6.** Bayesian predictions for custom migration models between GSMR and FC regions of the Gulf Stream using Migrate-N. The best (most likely) population connectivity model based on each gene region is shown in bold. Abbreviations: Bezier Log Marginal Likelihood (*LML*); Log Bayes Factor (*LBF*).

| Barcode | Model hypothesis | *LML* | *LBF* | Model probability | Rank choice |
|---|---|---|---|---|---|
| COI | Full | **−14 664.99** | **0.00** | **1.00** | **1** |
| | FC to GSMR | −14 786.74 | 121.75 | 0.00 | 4 |
| | GSMR to FC | −14 680.91 | 15.92 | 0.00 | 2 |
| | Panmictic | −14 713.12 | 48.13 | 0.00 | 3 |
| CYB | Full | −798.85 | 5.32 | 0.00 | 2 |
| | FC to GSMR | **−793.53** | **0.00** | **1.00** | **1** |
| | GSMR to FC | −832.78 | 39.25 | 0.00 | 3 |
| | Panmictic | −836.34 | 42.81 | 0.00 | 4 |
| COI + CYB | Full | −1887.23 | 2.14 | 0.00 | 2 |
| | FC to GSMR | **−1885.09** | **0.00** | **1.00** | **1** |
| | GSMR to FC | −1896.48 | 11.39 | 0.00 | 3 |
| | Panmictic | −1904.57 | 19.48 | 0.00 | 4 |

marked diel vertical migration (Mauchline, 1980; Kaartvedt, 2010; Lowe *et al.*, 2018). Both species share small nucleotide diversities, large haplotype diversity, and departures from neutral expectations. In comparison with *S. elongatum*, *M. norvegica* exhibited lower variation of COI ($\theta_\pi = 0.0038$; $h_\mathrm{d} = 0.68$) than CYB ($\theta_\pi = 0.0182$; $h_\mathrm{d} = 0.91$) and no evidence of genetic differentiation among samples from the NW Atlantic Ocean (Bucklin *et al.*, 1997), although the species showed structure across its entire range (Patarnello *et al.*, 2010).

## Implications for global-scale patterns of euphausiid diversity

The genetic differentiation of *S. elongatum* populations over a portion of the Gulf Stream system contrasts with the lack of significant differentiation based on the COI barcode region of populations of globally-distributed *Stylocheiron* species. Several species of *Stylocheiron,* including *S. elongatum*, have extensive biogeographical distributions extending over multiple ocean basins; several warm-water euphausiid species occur in all of the Atlantic, Pacific, and Indian Oceans. A possible explanation for lack of genetic structuring of global-scale populations of marine zooplankton species, including *Stylocheiron*, is the power of purifying selection, which eliminates even slightly-disadvantageous mutations and may be especially effective in extremely large populations (Nei, 1987; Hughes, 2005), which are typical of marine zooplankton (Peijnenburg and Goetze, 2013). This conclusion is consistent with studies of impacts of selection on genetic diversity, including nucleotide frequencies in protein-coding genes, of marine organisms (Plough, 2016; Waples, 2016). COI and other widely-used marker genes are useful tools that will continue to provide insights into population genetic patterns and processes of zooplankton at local-to-global scales (Bucklin et al., 2011, 2021), but clearly population genomic approaches applied to samples collected across the extensive biogeographical distributions of marine zooplankton species will be key to new discoveries.

## Conclusions

Patterns of variation of the mitochondrial COI barcode region were examined within and among eight species of the euphausiid genus, *Stylocheiron*. Most species clustered together with significant bootstrap values, despite their extensive geographic ranges spanning multiple ocean basins. A primary exception was evidence of a distinct population and likely cryptic species of *S. affine* in the Red Sea. COI also showed little evidence of genetic diversity or structure within species of *Stylocheiron*, despite their circumglobal distributions. This finding is consistent with the hypothesis of purifying selection acting to reduce genetic diversity of species with extremely large population sizes.

The mesopelagic euphausiid, *S. elongatum*, was sampled from the FC and GSMR of the North Atlantic Ocean during cruises in February and April, 1993. Analysis of DNA sequence variation of mitochondrial COI and CYB for identified specimens showed small nucleotide and large haplotype diversities, and marked departures from expectations of neutral evolution. Based on COI variation, *S. elongatum* showed evidence of genetic differentiation within and among samples within regions; COI + CYB showed divergence between the FC and GSMR regions. These patterns of genetic diversity support our hypothesis of population divergence driven by selection, with persistent genetic structure made possible by the species' deep distribution and lack of vertical migration behavior, which slow advective transport in the Gulf Stream System and reduce mixing of populations in the North Atlantic Ocean.

## Supplementary data

Supplementary material is available at the *ICESJMS* online version of the manuscript.

## Author contributions

Designed research: AB, PHW; Performed research: AF, SS; Analyzed data: AB, JMQ, LBB; Wrote the paper: AB, PHW

## Data availability

The data underlying this article are available in the GenBank Nucleotide Database (https://www.ncbi.nlm.nih.gov/nucleotide/) and the MetaZooGene Barcode Atlas and Database (MZGdb; https://metazoogene.org/MZGdb) and can be accessed with GenBank Accession Numbers provided in Supplementary Tables S1 and S2.

## Acknowledgements

The efforts and experience of the Captains and crews of *R/V Oceanus* (Cruise OCE-258) and *R/V Calanus* (Cruise CA-9303) were invaluable for this effort. We gratefully acknowledge the assistance during the research cruises of Karen Garrison and Frank Bub (previously at the University of New Hampshire, USA) and the laboratory contributions of James J. Pierson (now at the University of Maryland). Todd O'Brien (NOAA Fisheries, USA) provided expert guidance for use of the MetaZooGene Barcode Database and Atlas for accessing data and mapping locations. This publication resulted in part from support to SCOR WG 157 from the U.S. National Science Foundation (Grant number OCE-1840868) to the Scientific Committee on Oceanic Research (SCOR) and from funds contributed by national SCOR committees. The authors acknowledge contributions from the Working Group on Integrated Morphological and Molecular Taxonomy (WGIMT) of the International Council for the Exploration of the Sea (ICES). Funding to A. Bucklin was provided by the Biological Oceanography Program of the Office of Naval Research (Grant numbers N00014-93-1–0178 and N00014-1-96-0302).

## References

Aarbakke, O. N., Bucklin, A., Halsband, C., and Norrbin, F. 2014. Comparative phylogeography and demographic history of five sibling species of *Pseudocalanus* (Copepoda: calanoida) in the North Atlantic Ocean. Journal of Experimental Marine Biology and Ecology, 461: 479–488.

Altschul, S. F., Madden, T. L., Schäffer, A. A., Zhang, J., Zhang, Z., Miller, W., and Lipman, D. J. 1997. Gapped BLAST and PSI-BLAST: a new generation of protein database search programs. Nucleic Acids Research, 25: 3389–3402.

Avise, J. C. 2000. Phylogeography: The History of Formation of Species. Harvard University Press, Cambridge. 447p.

Avise, J. C. 2004. Molecular Markers, Natural History and Evolution, 2nd edn. Sinauer Associates, Sunderland, MA. 684p.

Beerli, P., and Felsenstein, J. 2001. Maximum likelihood estimation of a migration matrix and effective population sizes in n subpopulations by using a coalescent approach. Proceedings of the National Academy of Sciences, 98: 4563–4568.

Beerli, P. 2016. Migrate Documentation, Version 4.0. Florida State University Press, Tallahassee, FL, 58.

Brinton, E. 1962. The distribution of Pacific euphausiids. Bulletin of the Scripps Institution of Oceanography, 8: 51–270.

Brinton, E., Ohman, M. D., Townsend, A. W., Knight, M. D., and Bridgeman, A. L. 1999. Euphausiids of the World Ocean, Ver. 1.0. CD-ROM for Macintosh. Springer-Verlag, Berlin.

Bucklin, A., LaJeunesse, T. C., Curry, E., Wallinga, J., and Garrison, K. 1996. Molecular genetic diversity of the copepod, *Nannocalanus minor*: genetic evidence of species and population structure in the N. Atlantic Ocean. Journal of Marine Research, 54: 285–310.

Bucklin, A., Smolenack, S. B., Bentley, A. M., and Wiebe, P. H. 1997. Gene flow patterns of the euphausiid, *Meganyctiphanes norvegica*, in the N. Atlantic based on DNA sequences for mitochondrial cytochrome oxidase I and cytochrome b. Journal of Plankton Research, 19: 1763–1781.

Bucklin, A. 2000. Methods for population genetic analysis of zooplankton. *In* The ICES Zooplankton Methodology Manual, pp. 533–570. Harris, R. P., Huntley, M., Lenz, J., Skjoldal, H. R., and Wiebe, P. H. (Eds). International Council for the Exploration of the Sea. Academic press, London.

Bucklin, A., Wiebe, P. H., Smolenack, S. B., Copley, N. J., Beaudet, J. G., Bonner, K. G., Färber Lorda, J. *et al.* 2007. DNA barcodes for species identification of euphausiids (Euphausiacea, Crustacea). Journal of Plankton Research, 29: 483–493.

Bucklin, A., Steinke, D., and Blanco-Bercial, L. 2011. DNA barcoding of marine metazoa. Annual Review of Marine Science, 2011 3: 471–508.

Bucklin, A., DiVito, K., Smolina, I., Choquet, M., Questel, J. M., Hoarau, G., and O'Neill, R. J. 2018. Population genomics of marine zooplankton. *In* Population Genomics: Marine Organisms, pp. 61–102. Rajora, O. P., and Oleksiak, M. (Eds). Springer International Publ.

Bucklin, A., Peijnenburg, K. T. C. A., Kosobokova, K. N., O'Brien, T. D., Blanco-Bercial, L., Cornils, A., Falkenhaug, T. *et al.* 2021. Toward a global reference database of COI barcodes for marine zooplankton. Marine Biology, 168: 78.

Davis, C. S., and Wiebe, P. H. 1985. Macrozooplankton biomass in a warm-core Gulf Stream ring: time series changes in size structure, taxonomic composition, and vertical distribution. Journal of Geophysical Research, 90: 8871–8884.

Edgar, R. C. 2004. Muscle: a multiple sequence alignment method with reduced time and space complexity. Bmc Bioinformatics, 5, 113.

Endo, Y., and Wiebe, P. H. 2007. Temporal changes in euphausiid distribution and abundance in North Atlantic cold-core rings in relation to the surrounding waters. Deep Sea Research Part I: Oceanographic Research Papers. 54: 181–202.

Excoffier, L., and Lischer, H. E. L. 2010. Arlequin suite ver 3.5: a new series of programs to perform population genetics analyses under Linux and Windows. Molecular Ecology Resources, 10: 564–567.

Folmer, O., Black, M., Hoen, W., Lutz, R., and Vrijenhoek, R. 1994. DNA primers for amplification of mitochondrial cytochrome c oxidase subunit I from diverse metazoan invertebrates. Molecular Marine Biology and Biotechnology, 3: 294–299.

Gaube, P., and McGillicuddy, D. J. 2017. The influence of Gulf Stream eddies and meanders on near-surface chlorophyll. Deep Sea Research Part I: Oceanographic Research Papers, 122: 1–16.

Goetze, E., Andrews, K. R., Peijnenburg, K. T. C. A., Portner, E., and Norton, E. L. 2015. Temporal stability of genetic structure in a mesopelagic copepod. Plos ONE, 10: e0136087.

Harkins, G. W., D'Amato, M. E., and Gibbons, M. J. 2013. Self-maintaining or continuously refreshed? The genetic structure of *Euphausia lucens* populations in the Benguela upwelling ecosystem, Journal of Plankton Research, 35: 982–992.

Hastings, W. K. 1970. Monte Carlo sampling methods using Markov chains and their applications. Biometrika, 57: 97–109.

Heiderich, J., and Todd, R. E. 2020. Along-stream evolution of Gulf Stream volume transport. Journal of Physical Oceanography, 50: 2251–2270.

Holm, S. 1979. A simple sequentially rejective multiple test procedure. Scand. J. Stat., 6: 65–70.

Hughes, A. L. 2005. Evidence for abundant slightly deleterious polymorphisms in bacterial populations. Genetics, 169: 533–538.

Kaartvedt, S. 2010. Diel vertical migration behaviour of the northern krill (*Meganyctiphanes norvegica* Sars). Advances in Marine Biology, 57: 255–275.

Kocher, T. D., Thomas, W. K., Meyer, A., Edwards, S. V., Pääbo, S., Villablanca, F. X., and Wilson, A. C. 1989. Dynamics of mitochondrial DNA evolution in animals: amplification and sequencing with conserved primers. Proceedings of the National Academy of Sciences, 86: 6196–6200.

Kulagin, D. N., Lunina, A. A., Simakova, U. V., and Vereshchaka, A. L. 2021. Progressing diversification and biogeography of the mesopelagic *Nematoscelis* (Crustacea: euphausiacea) in the Atlantic, ICES Journal of Marine Science, 2021: fsab028

Kumar, S., Stecher, G., and Tamura, K. 2016. MEGA7: molecular Evolutionary Genetics Analysis version 7.0 for bigger datasets. Molecular Biology and Evolution, 33: 1870–1874.

Librado, P., and Rozas, J. 2009. DNASP V5: a software for comprehensive analysis of DNA polymorphism data. Bioinformatics, 25: 1451–1452.

Lowe, M. R., Lawson, G. L., and Fogarty, M. J. 2018. Drivers of euphausiid distribution and abundance in the Northeast U.S. Shelf Large Marine Ecosystem. ICES Journal of Marine Science, 75: 1280–1295.

Mauchline, J. 1980. The biology of mysids and euphausiids. Part 2. The biology of euphausiids. Advances in Marine Biology, 18: 372–623.

Meinen, C. S., and Luther, D. S. 2016. Structure, transport, and vertical coherence of the Gulf Stream from the Straits of Florida to the Southeast Newfoundland Ridge. Deep Sea Research Part I: Oceanographic Research Papers, 112: 137–154.

Meunier, T., Pallàs-Sanz, E., Tenreiro, M., Portela, E., Ochoa, J., Ruiz-Angulo, A., and Cusí, S. 2018. The vertical structure of a loop current eddy. Journal of Geophysical Research: Oceans, 123: 6070–6090.

Miyamoto, H., Machida, R. J., and Nishida, S. 2012. Global phylogeography of the deep-sea pelagic chaetognath *Eukrohnia hamata*. Progress in Oceanography, 104: 99–109.

Nei, M. 1987. Molecular Evolutionary Genetics. Columbia University Press, New York.

Palumbi, S. R. 1996. Nucleic acids II: the polymerase chain reaction. Chapter 7, *In* Molecular Systematics, 2nd edn. pp. 205–248. Hillis, D. M., Moritz, C., and Mable, B. K. (Eds). Sinauer Assoc., Inc., Sunderland, MA.

Patarnello, T., Papetti, D., and Zane, L. 2010. Genetics of Northern Krill (*Meganyctiphanes norvegica* Sars). *In* Advances in Marine Biology, 57, pp. 41–57. Tarling, G. A. (Ed). Academic Press.

Peijnenburg, KTCA., and Goetze, E. 2013. High evolutionary potential of marine zooplankton. Ecology and Evolution, 3: 2765–2781.

Plough, LV. 2016. Genetic load in marine animals: a review. Current Zoology. 62: 567–579.

Questel, J. M., Blanco-Bercial, L., Bucklin, A., and Hopcroft, R. R. 2016. Phylogeography and connectivity of four sibling species of *Pseudocalanus* (Copepoda: calanoida) in the North Pacific and Arctic Ocean. Journal of Plankton Research, 38: 610–623.

Raupach, M. J., and Redulovici, A. E. 2015. Looking back on a decade of barcoding crustaceans. Zookeys, 539: 53–81

Rozas, J., Ferrer-Mata, A., Sánchez-DelBarrio, J. C., Guirao-Rico, S., Librado, P., Ramos-Onsins, S. E., and Sánchez-Gracia, A. 2017. DnaSP 6: DNA sequence polymorphism analysis of large data sets. Molecular Biology and Evolution, 34: 3299–3302.

Saitou, N., and Nei, M. 1987. The neighbor-joining method: a new method for reconstructing phylogenetic tree. Molecular Biology and Evolution, 4: 406–425.

Sanford, E., and Kelly, M. W. 2011. Local adaptation in marine invertebrates. Annual Review of Marine Science, 3: 509–535.

Tajima, F. 1989. Statistical method for testing the neutral mutation hypothesis by DNA polymorphism. Genetics, 123: 585–595.

Tamura, K. 1992. Estimation of the number of nucleotide substitutions when there are strong transition-transversion and G+C-content biases. Molecular Biology Evolution, 9: 678–687.

Tobe, S. S., Kitchener, A. C., and Linacre, A. M. T. 2010. Reconstructing mammalian phylogenies: a detailed comparison of the cytochrome b and cytochrome oxidase subunit I mitochondrial genes. Plos ONE, 5: e14156.

Vereshchaka, A. L., Kulagin, D. N., and Lunina, A. A. 2019. A phylogenetic study of krill (Crustacea: euphausiacea) reveals new taxa and co-evolution of morphological characters. Cladistics, 35: 150–172.

Waples, RS. 2016. Making sense of genetic estimates of effective population size. Molecular Ecology, 25: 4689–4691.

Wiebe, P. H., and Flierl, G. R. 1983. Euphausiid invasion/dispersal in Gulf Stream cold-core rings. Marine and Freshwater Research, 34: 625–652.

Wiebe, P. H., Morton, A. W., Bradley, A. M., Backus, R. H., Craddock, J. E., Cowles, T. J., Barber, V. A. *et al.* 1985. New developments in the MOCNESS, an apparatus for sampling zooplankton and micronekton. Marine Biology, 87: 313–323.

Wiebe, P. H., Copley, N. J., and Boyd, S. H. 1992. Coarse-scale horizontal patchiness and vertical migration of zooplankton in Gulf Stream warm-core ring 82-H. Deep Sea Research Part A. Oceanographic Research Papers, 39: S247–S278.

Wiebe, P. H., Bucklin, A., Kaartvedt, S., Røstad, A., and Blanco-Bercial, L. 2016. Vertical distribution and migration of euphausiid species in the Red Sea. Journal of Plankton Research, 38: 888–903.

Wishner, K. F., and Allison, S. K. 1986. The distribution and abundance of copepods in relation to the physical structure of the Gulf Stream. Deep Sea Research Part A. Oceanographic Research Papers, 33: 705–731.

WoRMS Editorial Board. 2021. World Register of Marine Species. Available from: http://www.marinespecies.org at VLIZ. (last accessed 9 May 2021). doi:10.14284/170.

Worthington, L. V. 1976. On the North Atlantic circulation. *In* The Johns Hopkins Oceanogr. Studies, No. 6, Johns Hopkins University Press, Baltimore. pp. 110.

*Handling editor: William Grant*